Chapter

DIFFUSING ACOUSTIC WAVE TRANSPORT AND SPECTROSCOPY

J.H. PAGE, M.L. COWAN
Dept. of Physics and Astronomy, University of Manitoba, Winnipeg, Manitoba, Canada, R3T 2N2

PING SHENG
Dept. of Physics, Hong Kong Univ. of Science & Technology, Clear Water Bay, Kowloon, Hong Kong

D.A. WEITZ
Dept. of Physics and Astronomy, University of Pennsylvania, Philadelphia, PA 19104-6396 U.S.A

Key words: Diffusion of acoustic waves, multiple scattering, energy velocity, Diffusing Acoustic Wave Spectroscopy.

Abstract: Measurements of the diffusive transport of ultrasonic waves have been performed to critically test the applicability of the diffusion approximation for multiply scattered sound. By performing these measurements over an extended range of frequencies, we have shown that the energy velocity of diffusing ultrasound is similar in magnitude and frequency dependence to the group velocity, giving a unified physical picture of the velocities of energy transport by both diffusive and ballistic wave pulses. This information on diffusive transport of ultrasound has facilitated the development of a new ultrasonic technique, Diffusing Acoustic Wave Spectroscopy (DAWS), for probing the dynamics of structured media. The feasibility and sensitivity of DAWS has been demonstrated by studying the motion of particles in fluidised suspensions, providing important new information on the velocity fluctuations and local strain rate of fluidised particles.

1. INTRODUCTION

Over the last two decades, there has been a considerable resurgence of interest in the propagation of classical waves through inhomogeneous materials that scatter the waves very strongly [1, 2]. Most of the experimental activity has focused, however, on light and microwaves, and it is only during the last few years that successful measurements of multiply scattered ultrasound have been performed. These ultrasonic experiments have lead to new insights into the nature of the diffusive propagation of classical waves, a simple approximation that has been extensively used to interpret a wide range of wave phenomena in strongly scattering media. In this paper, we will first review this recent progress in investigating the diffusive transport of ultrasonic waves, and then describe a new ultrasonic technique, Diffusing Acoustic Wave Spectroscopy, that takes advantage of this knowledge to probe the dynamics of the scattering particles themselves.

2. DIFFUSIVE TRANSPORT OF ACOUSTIC WAVES

To study the diffusive transport of ultrasonic waves, we have focussed mostly on a simple realisation of random strongly scattering materials consisting of randomly close packed solid glass spheres immersed in a fluid. In the intermediate frequency regime, where the ultrasonic wavelength is comparable with the size of the scatterers, the propagation is dominated by very strong multiple scattering due to the large solid-fluid impedance mismatch. In this regime, we have shown [3] that the transport of energy by the scattered waves is well described using the diffusion approximation, in which all phase information is neglected and the propagation is modelled as a random walk process. Within this approximation, the dynamic transport is described in terms of the wave diffusion coefficient $D = v_e l^*/3$, where v_e is the energy velocity, which corresponds to the average local velocity of energy transport in the diffusion process, and l^* is the transport mean free path, or the distance the waves must propagate until their direction is randomised. To critically test the validity of the diffusion approximation for multiply scattered ultrasound, we have performed a series of transmission measurements over an extended range of frequencies f and sample thicknesses L using both pulsed and quasi-continuous-wave techniques [3, 4]. These measurements were performed in a water tank by placing slab-shaped samples containing the random scatterers between a plane wave generating transducer and a miniature hydrophone detector, which was small enough to measure the transmitted pressure field in a single (near-field) coherence area, or speckle. The transmitted diffusive flux was then

measured by ensemble averaging the intensity over many independent speckles. By fitting the predictions of the diffusion model to our data, we measured the diffusion coefficient in the pulsed experiments and the transport mean free path in the cw experiments. Results for the frequency dependence of D and l^* are shown in Figs. 1(a) and (b), where we plot D/a and l^*/a as a function of the normalised frequency $k_w a$, where $k_w = 2\pi f/v_w$ is the ultrasonic wave vector in water, f is the frequency, and v_w is the sound velocity in water. We find that the diffusion coefficient D shows a pronounced variation with frequency in the strong scattering regime where $k_w a > 2$, while the transport mean free path l^* does not. In Fig. 1(b), the transport mean free path (solid symbols) is compared with the scattering mean free path l_s (open symbols), measured independently from the attenuation of the ballistic pulse intensity, $I_{ballistic} = I_0 \exp[-L/l_s]$, that travels though the sample without being scattering out of the forward direction. At the low end of the intermediate frequency regime, $k_w a \leq 4$, we find $l^* \sim l_s$, indicating that even though the scattering is very strong, it is nearly isotropic on average. At higher frequencies, however, l_s becomes even shorter while l^* remains roughly equal to the diameter of the scatterers.

Since we have measured both D and l^*, we can also use these data to determine the energy velocity from the ratio $v_e = 3D/l^*$ (solid symbols in Fig. 1(c)). Like D, v_e exhibits a strong frequency dependence, reflecting a substantial slowing down of wave propagation over much of this frequency range due to scattering in the medium. Insight into this behaviour is obtained by comparing the energy velocity with the group velocity v_g [4-6], shown by the open symbols in Fig. 1(c). As seen in this figure, we find experimentally that v_e and v_g are remarkably similar in magnitude and frequency dependence, a result that was not expected from earlier theoretical work for light [7-9]. These data suggest a simple physical picture for v_e based on our observation in acoustics that a close connection must exist between v_e and v_g, the velocities which describe the transport of energy by diffusive and ballistic waves respectively. Even in the forward direction, the transport of energy by wave pulses is strongly affected by the scattering, which leads to a large scattering delay at frequencies near the minima of v_g. It is reasonable to expect that wave pulses scattered through a non-zero scattering angle will experience a similar, but not identical, scattering delay, so that in this picture of energy transport by wave pulses, v_e and v_g should exhibit similar behaviour. Thus v_e should be simply related to v_g by the additional angle-averaged scattering delay of the scattered waves.

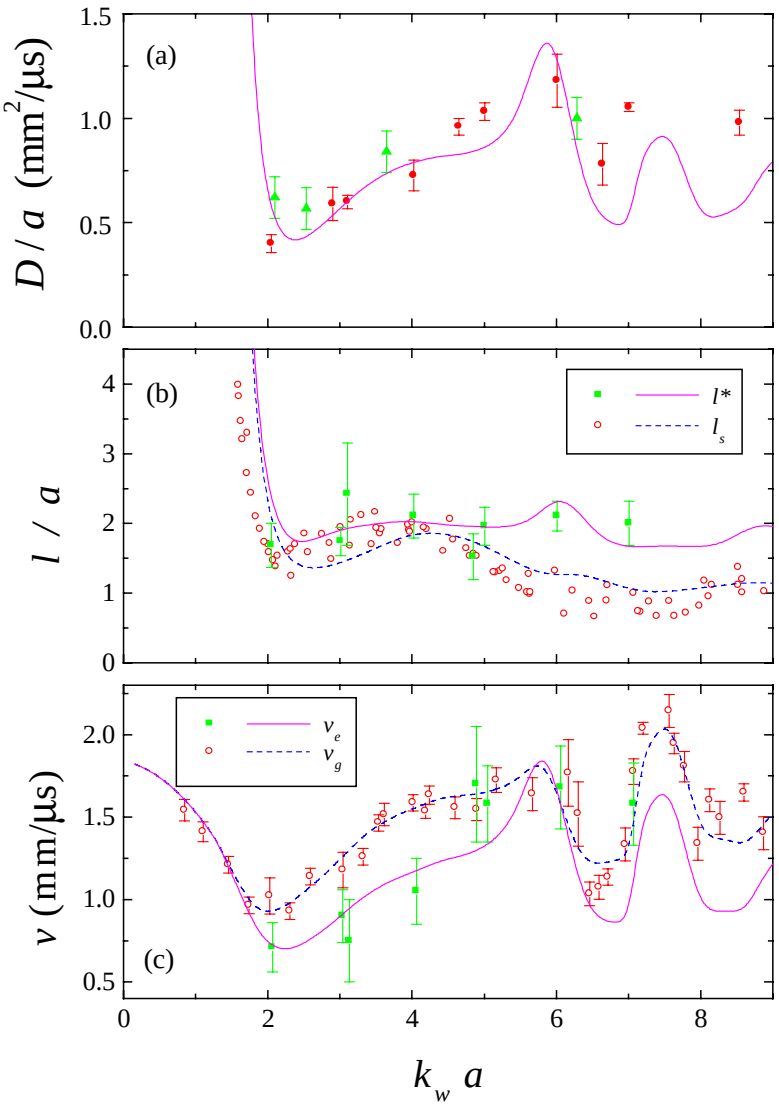

Figure 1. Frequency dependence of (a) the diffusion coefficient, (b) the transport and scattering mean free paths, and (c) the energy and group velocities of ultrasonic waves propagating through a randomly close packed suspension of glass spheres in water.

We are able to explain these results quantitatively using a new effective medium model, which is based on a spectral function approach [10-12]. This approach gives a simple criterion for determining the dispersion relation of the medium that is not only physically plausible but can be shown on general grounds to be very accurate so long as the mean free path is not

so short that $kl_s < 2$. Even though this model was developed initially to describe only the coherent ballistic component, its success in describing the behaviour of the group velocity [5] has formed a basis for extending the model to determine the energy velocity of diffusive acoustic waves [4]; this has been accomplished by explicitly accounting for the additional scattering delay experienced by the scattered wave pulse. In this model, the basic scattering unit is taken as a coated elastic sphere embedded in an effective medium, whose properties are determined by identifying the frequencies and wave vectors of the coherent propagating modes from the peaks in the spectral function. The complex scattering amplitude for the coated elastic sphere is then used to determine the angular dependence of the phase shift relative to the forward direction for each frequency component of a wave pulse, allowing the additional scattering delay of the wave pulse to be calculated as a function of scattering angle. The intensity-weighted angular average of this additional scattering delay, Δt_{ave}, allows the energy velocity to be calculated from the group velocity as $v_e = v_g/(1+\delta_m)$, where $\delta_m = \Delta t_{ave} v_g/l^*$. The predictions of this model for the velocities and mean free paths of diffusive and ballistic propagation are shown by the solid and dashed curves respectively in Fig. 1. Excellent quantitative agreement is seen not only for these quantities but also for the diffusion coefficient, $D = v_e l^*/3$. Thus accurate calculations of D can be obtained from a single Green's function approach to determine v_e and l^*, rather than having to evaluate the configurational average of the product of two Green's functions, as is normally done to determine the properties of the diffuse intensity.

Furthermore, we are able to identify the mechanisms responsible for the remarkably slow velocities by calculating the ultrasonic energy density, both inside the scatterers and in the surrounding fluid [6]. We have demonstrated that there are important contributions both from resonant scattering by the glass spheres, where energy is trapped within the solid scatterers, and from tortuosity effects, where the wave energy is largely confined to the tortuous fluid pathways. Thus we are able to obtain a microscopic physical picture of energy transport by diffusive acoustic waves in these strongly scattering media - an important step in facilitating both the search for acoustic wave localisation in more strongly scattering samples and the development of a novel probes of multiply scattering materials.

3. DIFFUSING ACOUSTIC WAVE SPECTROSCOPY

In the presence of strong multiple scattering, traditional ultrasonic imaging techniques break down, motivating the use of other approaches to learn about the structure and dynamics of strongly scattering materials. We

have exploited our understanding of the diffusive transport of ultrasound in slurries to develop a new technique for probing the dynamics of moving scatterers. This technique, which we call Diffusing Acoustic Wave Spectroscopy (DAWS) by analogy with Diffusing Wave Spectroscopy using light [13, 14], determines the relative motion of the scattering particles from the temporal fluctuations of the scattered ultrasonic waves. To demonstrate the feasibility and excellent sensitivity of DAWS, we have used this technique to study the dynamics of fluidised suspensions of glass beads in water-glycerol mixtures, where the particles are supported by flowing the fluid upward to counteract gravity-induced sedimentation. Even though the average velocity of the particles is zero, they are far from stationary, and understanding their dynamics remains a challenging and interesting problem because of the complexity of the many-body hydrodynamic interactions that are involved.

Since pulsed techniques are often relatively easy to implement in ultrasonics, we describe pulsed DAWS here, although we have also performed continuous wave DAWS in situations where a narrow frequency bandwidth was important for a quantitative interpretation of the data. Fig. 2(a) shows the transmitted ultrasonic field in a single speckle when the input pulse, shown on the left, is incident on the suspension. The central frequency in the pulse was 2.35 MHz, at which frequency the transport mean free path $l^* = 1.0$ mm for a volume fraction of glass beads equal to 40%. This value of the mean free path corresponds very closely to the average centre-to-centre distance between the particles, an example of how very strong the scattering is in these experiments. On subsequent repetitions of the input pulse, the measured field profile undergoes fluctuations due to the motion of the scattering particles, as illustrated by the thin dotted line in Fig. 2(a), which shows the field at a later time. The simplest way to record these field fluctuations is to use a boxcar to measure the field at a fixed sampling time t_s after the incident pulse starts to diffuse through the suspension, and to digitise the boxcar output on a digital oscilloscope. To measure the true field at this sampling time, the gate on the boxcar is set at a very short time interval, typically about $1/20^{th}$ of the ultrasonic period. Thus we are able to measure the fluctuations of the multiply scattered fields at a fixed path length of diffusing sound $s = v_e\, t_s$ though the sample. A short segment of these field fluctuations, measured at a sampling time $t_s = 27.8$ μs in the diffusion profile, is illustrated in Fig. 2(b), where the time interval between data points is set by the pulse repetition rate, typically 1 kHz in our experiments. The full temporal record of the field fluctuations $F(t)$ generally extended to approximately 130,000 points or pulse repetitions, and was repeated 50 times to further improve the statistics.

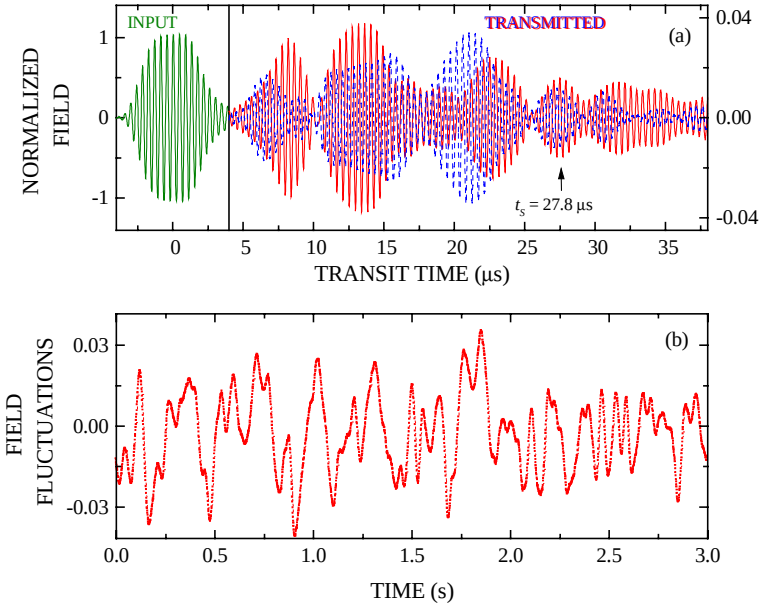

Figure 2. (a) Transmitted ultrasonic field in a single speckle (solid curve) compared with the transmitted field at a later time (thin dotted curve). The input pulse is shown on the left. (b) Field fluctuations at the sampling time t_s = 27.8 μs in the diffusion profile.

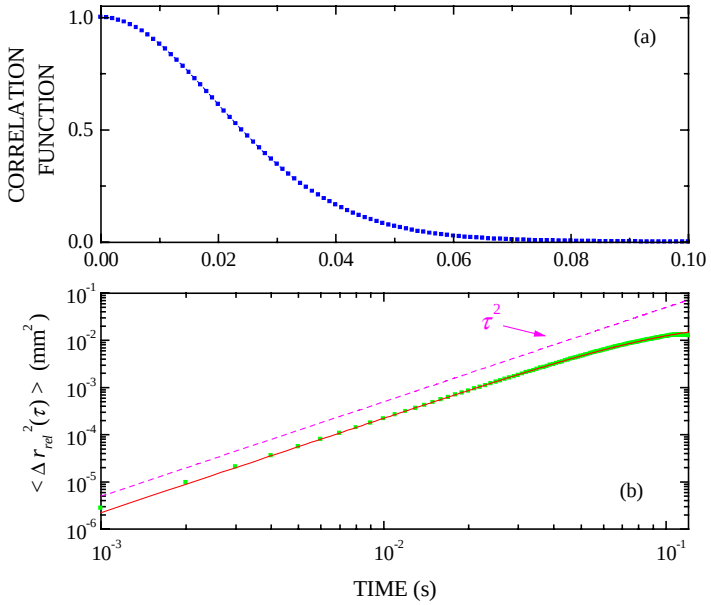

Figure 3. (a) Temporal auto-correlation function of the field fluctuations. (b) Mean square relative displacement of the particles as a function of time.

To investigate the motion of the particles, we first determine the temporal auto-correlation function $g_1(\tau)$ of the measured field fluctuations,

$$g_1(\tau) = \frac{F(t)F^*(t+\tau)\,dt}{\left|F(t)\right|^2 dt}, \tag{1}$$

using a Fourier transform technique. Typical results for the field correlation function are shown in Fig. 3(a), where $g_1(\tau)$ is calculated from the field fluctuations illustrated in Fig. 2(b). The decay of $g_1(\tau)$ is determined by the total phase change of diffusing sound for $n = s/l^*$ sequential scatterings from the moving particles, where $n \approx 50$ for the data shown in Fig. 3(a). This phase change can be written as

$$\Delta\phi^{(n)}(\tau) = \sum_p^n \left[\boldsymbol{k}_p \cdot \left(\Delta\boldsymbol{r}_{p+1}(\tau) - \Delta\boldsymbol{r}_p(\tau) \right) \right] \tag{2}$$

where $\boldsymbol{k}_p$ is the wave vector of the wave scattered from the p^{th} to the $(p+1)^{\text{th}}$ particle, and $\Delta\boldsymbol{r}_{rel,p}(\tau) = \Delta\boldsymbol{r}_{p+1}(\tau) - \Delta\boldsymbol{r}_p(\tau)$ is their relative displacement during the time interval τ. By calculating the ensemble-averaged contributions of the phase changes from all paths containing n scattering events, the pulsed DAWS correlation function can be written

$$\begin{aligned} g_1(\tau) &= \left\langle \exp\left[-i\Delta\phi^{(n)}(\tau) \right\rangle \right. \\ &\approx \exp\left[-(s/l^*) k^2 \left\langle \Delta r_{rel}^2(\tau) \right\rangle / 6 \right] \end{aligned} \tag{3}$$

where $\langle \Delta r_{rel}^2(\tau) \rangle$ is the mean square displacement of the particles relative to their neighbours a distance l^* away [15]. The second line of Eq. (3) is strictly valid only when there is no correlation between the magnitude of the component of $\Delta\boldsymbol{r}_{rel,p}(\tau)$ along $\boldsymbol{k}_p$ and the angle between these two vectors, but is expected to be a good approximation for the non-uniform motion typical of the fluidised suspensions investigate here. For correlated motion, only a fraction of the full $\langle \Delta r_{rel}^2(\tau) \rangle$ is measured in DAWS, one extreme example being the case of pure rotations, which give no contribution to the decay of $g_1(\tau)$, since DAWS is sensitive only to the component of $\Delta\boldsymbol{r}_{rel}(\tau)$ parallel to the scattering wave vector between adjacent scattering events. In general, the measured $\langle \Delta r_{rel}^2(\tau) \rangle$ can be written in terms of the strain tensor $\varepsilon_{ij}(\tau) = \frac{1}{2}(\partial_i u_j(\tau) + \partial_j u_i(\tau))$ as [16, 17]

$$\left\langle \Delta r_{rel,\,meas}^2(\tau) \right\rangle = \bar{\varepsilon}^2(\tau)\, l^{*2} = \tfrac{2}{5} l^{*2} \left[\left\langle \left(\varepsilon_{ii}(\tau) \right)^2 \right\rangle + 2 \sum_{i,j} \left\langle \varepsilon_{ij}^2(\tau) \right\rangle \right] \quad (4)$$

Here $\boldsymbol{u}(\tau) = \Delta\boldsymbol{r}(\tau)$, and $\bar{\varepsilon}$ is the average strain.

We use the methods outlined in section 2 to measure v_e, l^* and k from separate diffusive and ballistic ultrasound propagation experiments [3-6], enabling us to determine $\langle \Delta r_{rel}^2(\tau)$ and $\bar{\varepsilon}(\tau)$ by inverting Eq. (3) for $g_1(\tau)$. Typical results are shown in Fig. 3(b). This figure shows that the particles initially move in ballistic trajectories, $\langle \Delta r_{rel}^2(\tau) = \langle \Delta V_{rel}^2 \tau^2$, whose magnitude is given by the variance in the relative velocity of the particles $\langle \Delta V_{rel}^2$. Since l^* is essentially equal to the inter-particle separation at the frequency at which these measurements were made, DAWS can actually probe the relative motion of *adjacent* beads in the suspension, giving information on very short length scale motions that are difficult to obtain with other techniques. At later times, $\langle \Delta r_{rel}^2(\tau)$ crosses over to a weaker time dependence as the particle trajectories become altered by the interaction with neighbouring particles; this behaviour is well described by the empirical relation, $\langle \Delta r_{rel}^2(\tau) = \langle \Delta V_{rel}^2 \tau^2 / [1 + (\tau/\tau_\Delta)^2]$, shown by the solid curve in Fig. 3(b), allowing us to measure both $\Delta V_{rel} = [\langle \Delta V_{rel}^2]^{1/2}$ and the local fluctuation crossover time τ_Δ. Results for ΔV_{rel} and τ_Δ over a range of volume fractions between 0.18 and 0.5 are shown in Fig. 4; the system studied in this case is a suspension of 0.438-radius beads at a particle Reynolds number of 0.3. In Fig. 4, ΔV_{rel} is normalised by the Stokes velocity V_0, which corresponds to the sedimentation velocity of a single isolated particle in the fluid. The appreciable decrease in ΔV_{rel} with volume fraction ϕ reflects the comparable decrease in the average fluid flow speed, V_{flow}, required to counteract the sedimentation of the beads and keep them suspended. We find that the magnitude of the relative velocity fluctuations is remarkably large throughout this range of volume fractions, with $\Delta V_{rel} \sim V_{flow}$ at the length scale l^* at which the fluctuations are measured. From these fluctuations in the relative particle velocities, we can also determine the average local strain rate $\bar{\Gamma} = \bar{\varepsilon}/\tau \approx \Delta V_{rel}/l^*$, the first time that $\bar{\Gamma}$ has been probed on length scales of order the inter-particle separation in fluidised suspensions. Our results for $\bar{\Gamma}$ are shown in Fig. 5. Also shown is the average strain evaluated at the fluctuation crossover time τ_Δ, indicating that there are very substantial local rearrangements of the beads on the short time scales over which the beads move ballistically before interacting with their neighbours.

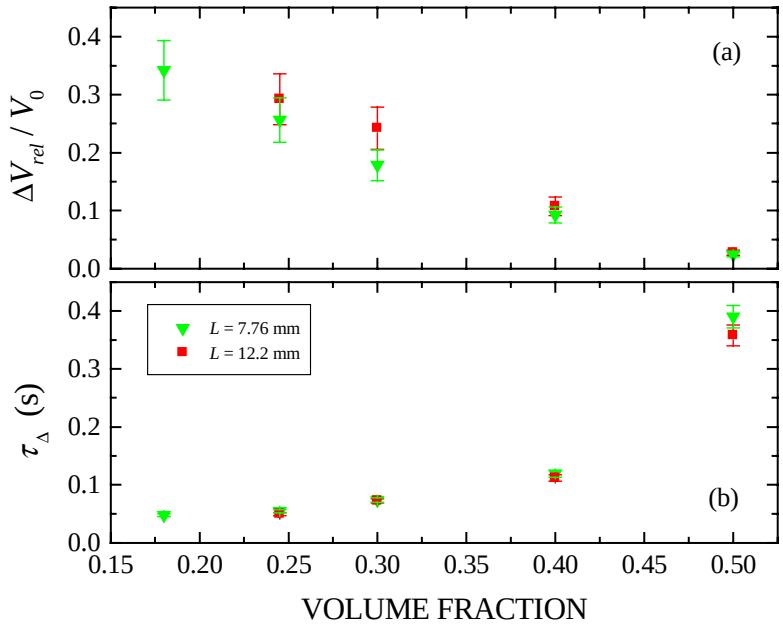

Figure 4. Volume fraction dependence of (a) the relative velocity fluctuations ΔV_{rel} normalised by the Stokes velocity, and (b) the local fluctuation crossover time τ_Δ.

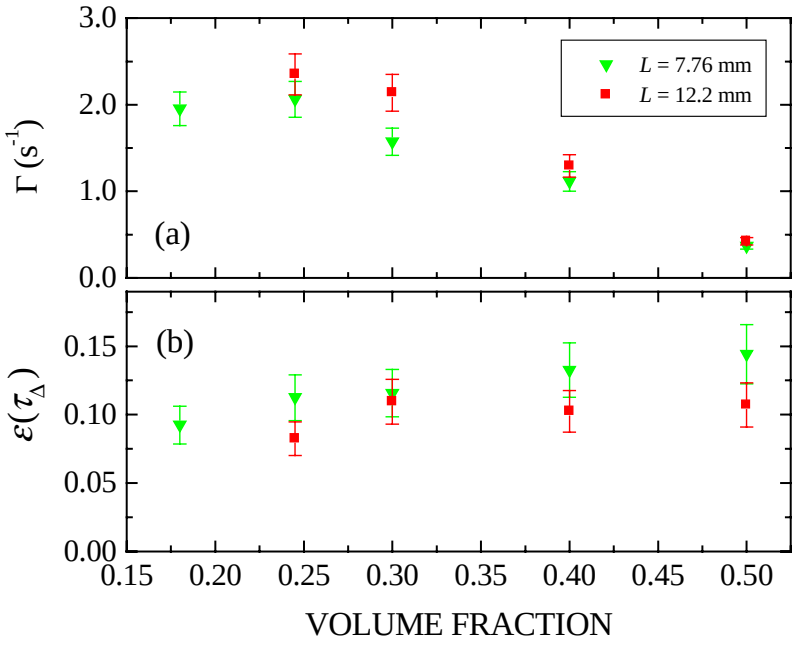

Figure 5. (a) The average strain rate $\bar{\Gamma}$ at the length scale l^*, which is comparable to the inter-particle spacing. (b) The average local strain $\bar{\varepsilon}$ at the crossover time τ_Δ.

To investigate the motion of the particles on longer length scales, we can lower the ultrasonic frequency so that $k_w a$ becomes less than 2, allowing the experiments to be repeated at larger values of l^* (c.f. Fig. 1). We find that the relative velocity fluctuations increase markedly with length scale, with the increase being well described by $\Delta V_{rel} \propto \sqrt{l^*}$, demonstrating that the velocity fluctuations are strongly correlated spatially at short length scales and early times [15]. Moreover, by combining DAWS with a novel implementation of Dynamic Sound Scattering (DSS) in the single scattering limit, we are able to estimate both the instantaneous and dynamic correlation lengths of the velocity fluctuations. Comparable large scale structures in the flow patterns of sedimenting suspensions have only recently be discovered [18], and only in the limit of creeping flow at very low particle Reynolds numbers, Re ~ 10^{-4}. Our new results demonstrate the power of these ultrasonic techniques to probe the dynamics of fluidised suspensions over a range of particle Reynolds numbers that are not accessible to light scattering methods because of the large particle sizes and length scales involved.

4. CONCLUSIONS

Recent progress in understanding the diffusive transport of ultrasonic waves has given new insights into the propagation of classical waves in strongly scattering media, and has shown how the energy velocity of diffusing acoustic waves may be understood in simple physical terms. This progress has enabled a new ultrasonic technique, called Diffusing Acoustic Wave Spectroscopy, to be developed. This technique avoids the limitations of traditional imaging experiments in strongly scattering materials and allows new information of the dynamics of the scattering particles to be obtained. We have shown that DAWS is ideally suited to investigating the dynamics fluidised suspensions with extremely high sensitivity. Our results show that there is considerable potential for gaining new information about the dynamics of structured media through the development of spectroscopic techniques such as DAWS, demonstrating that understanding the diffusive propagation of ultrasound is relevant for applications as well as fundamental studies in wave transport.

ACKNOWLEDGEMENTS

Acknowledgement is made to NSERC, NATO, Imperial Oil Ltd and the donors of the Petroleum Research Fund, administer by the ACS, for support of this research.

REFERENCES

[1] *Scattering and Localization of Classical Waves in Random Media*, edited by P. Sheng (World Scientific, Singapore, 1990).
[2] P. Sheng, *Introduction to Wave Scattering, Localization, and Mesoscopic Phenomena* (Academic Press, San Diego, 1995).
[3] J. H. Page, H. P. Schriemer, A. E. Bailey, and D. A. Weitz, Phys. Rev. E **52**, 3106 (1995).
[4] H. P. Schriemer, M. L. Cowan, J. H. Page, P. Sheng, Z. Liu, and D. A. Weitz, Phys. Rev. Lett. **79**, 3166 (1997).
[5] J. H. Page, P. Sheng, H. P. Schriemer, I. Jones, X. Jing, and D. A. Wietz, Science **271**, 634 (1996).
[6] M. L. Cowan, K. Beaty, J. H. Page, Z. Liu, and P. Sheng, Phys. Rev. E **58**, 6626 (1998).
[7] M. P. van Albada, B. A. van Tiggelen, A. Lagendijk, and A. Tip, Phys. Rev. Lett. **66**, 3132 (1991).
[8] B. A. van Tiggelen, A. Lagendijk, M. P. van Albada, and A. Tip, Phys. Rev. B **45**, 12233 (1992).
[9] B. A. van Tiggelen and A. Lagendijk, Europhys. Lett. **23**, 311 (1993).
[10] X. D. Jing, P. Sheng, and M. Y. Zhou, Phys. Rev. Lett. **66**, 1240 (1991).
[11] X. D. Jing, P. Sheng, and M. Y. Zhou, Phys. Rev. A **46**, 6513 (1992).
[12] P. Sheng, X. Jing, and M. Zhou, Physica (Amsterdam) **207A**, 37 (1994).
[13] G. Maret and P. E. Wolf, Z. Phys. B **65**, 409 (1987).
[14] D. J. Pine, D. A. Weitz, P. M. Chaikin, and E. Herbolzheimer, Phys. Rev. Lett. **60**, 1134 (1988).
[15] M. L. Cowan, J. H. Page, and D. A. Weitz, unpublished.
[16] M. L. Cowan, I. P. Jones, J. H. Page, and D. A. Weitz, unpublished.
[17] D. Bicout and R. Maynard, Physica A **199**, 387 (1993).
[18] P. N. Segrè, E. Herbolzheimer, and P. M. Chaikin, Phys. Rev. Lett. **79**, 2574 (1997).